Front. Phys. 11(1), 116804 (2016)
DOI 10.1007/s11467-015-0516-7

RESEARCH ARTICLE

Geometries and electronic structures of the hydrogenated diamond (100) surface upon exposure to active ions: A first principles study

Feng-Bin Liu (刘峰斌)[1,†], **Jing-Lin Li** (李景林)[2], **Wen-Bin Chen** (陈文彬)[1], **Yan Cui** (崔岩)[1], **Zhi-Wei Jiao** (焦志伟)[1], **Hong-Juan Yan** (阎红娟)[1], **Min Qu** (屈敏)[1], **Jie-Jian Di** (狄杰建)[1]

[1] *College of Mechanical and Material Engineering, North China University of Technology, Beijing 100144, China*
[2] *Changchun Institute of Optics, Fine Mechanics and Physics, Chinese Academy of Sciences, Changchun 130033, China*
Corresponding author. E-mail: [†]*fbliu@ncut.edu.cn*
Received July 29, 2015; accepted September 14, 2015

To elucidate the effects of physisorbed active ions on the geometries and electronic structures of hydrogenated diamond films, models of HCO_3^-, H_3O^+, and OH^- ions physisorbed on hydrogenated diamond (100) surfaces were constructed. Density functional theory was used to calculate the geometries, adsorption energies, and partial density of states. The results showed that the geometries of the hydrogenated diamond (100) surfaces all changed to different degrees after ion adsorption. Among them, the H_3O^+ ion affected the geometry of the hydrogenated diamond (100) surfaces the most. This is well consistent with the results of the calculated adsorption energies, which indicated that a strong electrostatic attraction occurs between the hydrogenated diamond (100) surface and H_3O^+ ions. In addition, electrons transfer significantly from the hydrogenated diamond (100) surface to the adsorbed H_3O^+ ion, which induces a downward shift in the HOMO and LUMO energy levels of the H_3O^+ ion. However, for active ions like OH^- and HCO_3^-, no dramatic change appears for the electronic structures of the adsorbed ions.

Keywords active ions, diamond surface, adsorption, electronic structure

PACS numbers 68.43.Bc, 68.47.Fg

1 Introduction

Diamond films exhibit a high surface conductivity after exposure to hydrogen plasma, a phenomena first discovered by Landstrass and Ravi in 1989 [1]. Because of this intriguing behavior, along with intrinsic biocompatibility, excellent chemical inertness, a wide electrochemical window, and good thermal conductivity, diamond films have attracted much attention. Based on these various attributes, some electronic and bioelectronic devices based on hydrogenated diamond films have been developed in recent years [2, 3].

The high surface conductivity of hydrogenated diamond films was initially attributed to shallow surface acceptors, which may arise from surface C-H moieties [4] or subsurface hydrogen atoms [5]. However, many subsequent experimental and theoretical studies failed to support this hypothesis [6–8]. Consequently, a "transfer doping model" proposed by Maier [9] is widely used to interpret the surface high conductivity of the hydrogenated diamond film. The model presumes that hydrogen termination is necessary but not sufficient for high surface conductivity. Instead, a thin water layer physically adsorbed on the hydrogenated diamond surface, which effectively constructs a tiny electrochemical system, is essential for high surface conductivity. Electron transfer would consequently occur at the interface between the hydrogenated diamond surface and the active ions in the water layer. The active ions in the thin water layer could include HCO_3^- [9, 10], H_3O^+ [9, 11], and so on, which are normally produced when certain gas molecules such as CO_2, O_2, or N_2 dissolve in water. Based on this "transfer doping model," some high surface conductivity phenomena for several different molecules physisorbed on hydrogenated diamond surfaces when exposed to air were well interpreted [11, 12]. However, the mechanism of electron transfer between the various active ions in the water layer

and the hydrogenated diamond surface is far from clarified. The effects of the adsorbed active ions on the surface conductivity of the hydrogenated diamond film are worth investigating explicitly so as to guide the development of higher sensitivity ion sensors.

In this work, models of the original hydrogenated (100) diamond surface and the hydrogenated (100) diamond surfaces individually adsorbed with HCO_3^-, H_3O^+, and OH^- ions were established. The selected HCO_3^-, H_3O^+, and OH^- ions are all common active ions existing in the adsorbed water layer [9–11]. The equilibrium geometries, adsorption energy, and partial density of states (PDOS) corresponding to different adsorption models were studied by using the first-principles method based on density functional theory. According to the calculation results, the effects of the adsorbed active ions on the surface conductivity of the hydrogenated diamond film were discussed.

2 Computational methods

All calculations in this work were carried out using CASTEP codes based on density functional theory. The electron-ion interaction was described by ultrasoft pseudopotentials and general gradient approximation (GGA) by Perdew-Burke-Ernzerhof (PBE) was employed for the exchange-correlation potentials [13]. Optimization of the atomic coordinates continued until the total energy converged within 10^{-6} eV/atom. The iterative calculation of the Kohn-Sham eigenstates was terminated when the eigenvalues were converged within 10^{-6} eV/atom.

Monolayer hydrogen atoms adsorbed on diamond (100) surface with 2×1 reconstruction was adopted as the hydrogenated diamond (100) surface for its most stable configuration, as reported elsewhere [4, 6]. The diamond surfaces were modeled as a finite slab consisting of six layers, each having nine C atoms. At the top and bottom of the slab, the C atom layers were covered with one layer of hydrogen atoms. To avoid repulsive interactions, a vacuum layer with a 15 Å thickness of was adopted [14]. All of the atoms except the bottom two layers of C atoms were allowed to relax freely during calculations. To calculate the total energies of the adsorbed ions, the models of a single ion in a vacuum box with the size of 15×15×15 Å were constructed. For the models of adsorbates on the hydrogen-terminated diamond surface, the optimized ions physisorbed on the optimized 2×1 reconstruction diamond (100) surface were constructed. For the adsorption models, wave functions were expanded into plane waves up to a cutoff energy of 320 eV. Concerning the Brillouin-zone integrations, a 4×4×1 grid of Monkhorst-Pack k-point sampling was used. For the single ion, the wave functions with a cutoff energy of 340 eV and a gamma Monkhorst–Pack k-point sampling grid were adopted.

3 Results and discussion

Table 1 shows the equilibrium geometries of the hydrogenated diamond (100) surfaces after adsorption with different ions. C(100)-H, C(100)-H OH^-, C(100)-H HCO_3^-, and C(100)-H H_3O^+ represent the configurations of the original, OH^-, HCO_3^-, and H_3O^+ ion physisorbed onto a hydrogenated diamond (100) surface, respectively. The r_{CH} is the surface C-H bonding length and r_{dimer} represents the bonding length of the surface C-C dimer. The $\theta_{(H-C-C)}$ value represents the angle between the surface C-H bonding and the C-C dimer. The S_{ij} is the interlayer space distance between the neighboring i and j carbon layer. By using the calculation parameters mentioned above, the geometries of the original C(100)-H configuration quantitatively agree with those from other reports [4, 6, 15, 16]. This verifies the reliability of the calculations presented here. The calculation results revealed that compared with the original C(100)-H surface, the surface geometries all change to different degrees after adsorptions of various ions. The relaxation can extend to the top three carbon layers of the diamond surface. Among the values, the r_{CH} for all the ion-adsorbed diamond surfaces is in the range of 1.101 to 1.104 Å, which alters slightly compared to the original, non-ion adsorbed value (1.103 Å). For r_{dimer} and $\theta_{(H-C-C)}$, they are 0.002 Å and 0.109° larger for the C(100)-H OH^- than those of the original configuration, respectively. No change was seen for r_{dimer}, and $\theta_{(H-C-C)}$ is 0.138° larger for the C(100)-H HCO_3^- relative to those for the C(100)-H. In contrast, the r_{dimer} and the $\theta_{(H-C-C)}$ for C(100)-H H_3O^+ exhibits the most significant change, 0.004 Å longer and 0.359° larger than those of the original configuration, respectively. The relaxation of the interlayer spaces also shows a similar tendency. The significant change of configuration parameters for the hydrogenated diamond (100) surface reflects the strong relaxation after the H_3O^+ adsorption. It follows that much stronger interactions occurs between the hydrogenated diamond (100) surface and the H_3O^+ ion. As for the adsorbed ions, except for the intact structure of the OH^- ion, the configurations of the other two ions both vary to different extents after adsorption on hydrogenated diamond (100) surfaces; this arises from the various action forces from the hydrogenated diamond (100) surfaces.

To further elucidate the interactions between the hy-

Table 1 The geometries of hydrogenated diamond (100) surfaces adsorbed with different ions.

Configurations	C(100)-H	C(100)-H OH^-	C(100)-H HCO_3^-	C(100)-H H_3O^+
r_{CH}(Å)	1.103	1.104	1.101	1.102
r_{dimer}(Å)	1.622	1.624	1.622	1.626
$\theta_{(H-C-C)}$(°)	113.119	113.228	112.883	113.477
S_{12}(Å)	0.811	0.810	0.804	0.802
S_{23}(Å)	1.002	1.003	1.005	1.008

drogenated diamond (100) surface and the physisorbed ions, the adsorption energies between the surface and ions were also investigated according to the following formula [11]. In Eq. (1), $E_{surface}$ and $E_{adlayer}$ are the energies of the hydrogenated diamond (100) surface and individual ion, respectively. The $E_{surface/adlayer}$ parameter represents the total energy of adsorption in the system. The $\Delta E_{adsorption}$ represents the adsorption energy, which is the difference between the $E_{surface/adlayer}$ and the sum of the $E_{surface}$ and $E_{adlayer}$.

$$\Delta E_{adsorption} = E_{surface/adlayer} - (E_{surface} + E_{adlayer})$$

The adsorption energies corresponding to the C(100)-H OH^-, C(100)-H HCO_3^-, and C(100)-H H_3O^+ are 2.211 eV, 1.725 eV, and -5.558 eV, respectively. These results indicate that for the negatively charged ions the adsorption energies are positive, demonstrating a repulsive force between the hydrogenated diamond (100) surface and the adsorbed ions. In contrast, for the H_3O^+ ion, the adsorption energy is negative, revealing a strong electrostatic attraction between the hydrogenated diamond (100) surface and the adsorbed ion. This electrostatic attraction can be attributed to the negative electron affinity of the hydrogenated diamond (100) surface [17, 18], which would certainly repel ions of the same sign of electric charge and attract ions of the opposite electric charge. Among the three adsorption systems, the C(100)-H H_3O^+ model shows the strongest interactions between the hydrogenated diamond surface and the H_3O^+ ion. This result is quite consistent with that obtained from geometrical structure and is in good accordance with the literature [11]. Such strong interactions may result from extremely high electron transfer between the diamond (100) surface and the adsorbed H_3O^+ ion [12]. For the C(100)-H HCO_3^- and C(100)-H OH^- models, the strong repulsive forces probably cannot induce significant electron transfer between the hydrogenated diamond (100) surface and the adsorption ions.

To investigate the electron transfer between the hydrogenated diamond (100) surface and the adsorption ions, electron population analyses were studied. This analysis showed that, compared with the original total charge for the three adsorption ions (+1 for H_3O^+ ion, –1 for both HCO_3^- and OH^- ions), various electron transfers occur due to the different coulomb electrostatic forces from the hydrogenated diamond (100) surface. The sum charge differences before and after different ion adsorptions are –0.98e, 0.28e and 0.21e for H_3O^+, HCO_3^-, and OH^- ions, respectively. It followed that for the positive ion H_3O^+, the electron transfers from the hydrogenated diamond (100) surface to the adsorption ion. Conversely, for the negatively charged ions like HCO_3^- and OH^-, electron transfer occurs from the adsorption ions to the hydrogenated diamond (100) surface. 0.98e transferred from the hydrogenated diamond surface to the H_3O^+ ion, which is the highest magnitude among the three adsorption ions. This magnitude of electron transfer has obvious contributions from the calculated strongest electrostatic attraction between the interface of the hydrogenated diamond surface and the H_3O^+ ion [12]. However, our value for this interaction is much smaller than that of a previous report, which maybe be attributed to the mixed species in the adlayer used in the prior work [11]. The O_3 present in the adlayer used in this literature result may have significant contributions to the electron transfer between the hydrogenated diamond surface and the adlayer, which is reported in recent literature [19, 20]. Note that the electron count change of each atom for the negatively charged ions HCO_3^- and OH^- ions are all very slight. However, the electron count changes of each atom for the physisorbed H_3O^+ ion are relatively dramatic (Table 2). For the H_3O^+ ion, the atomic charges for three H atoms and one O atom are 0.65e and –0.95e, respectively. After adsorption on a hydrogenated diamond (100) surface, the atomic charges for the three H atoms decreases to 0.31e, approximately 52.3% lower than that of the isolated ion. However, the atomic charge for the O atom after adsorption decreases slightly to

Table 2 The detailed atomic charge changes for H_3O^+ ion after adsorption (Unit: e).

The composed atoms of H_3O^+ ion	Atomic charge of the individual H_3O^+ ion	Atomic charge of the adsorptive H_3O^+ ion	Atomic charge difference
H	0.65	0.31	–0.34
O	–0.95	–0.91	0.04

–0.91e. Thus, the electrons mainly transfer to the H atoms of the H_3O^+ ion from the hydrogenated diamond surface, resulting in hole accumulation in the diamond film subsurface.

Figures 1–3 are the PDOS for the OH^-, HCO_3^-, and H_3O^+ ions, respectively. In Figs. 1–3, (a) represents the PDOS of the individual ions, while (b) represents that of the adsorbed ions. These results show that after adsorption, the highest occupied molecular orbitals (HOMOs) of the OH^- and HCO_3^- ions alter little compared to the original non-adsorbed ions. For the lowest unoccupied molecular orbitals (LUMOs) of the two ions, besides slight changes of the electron density, the energy levels of the LUMOs shift upward; this might originate from the electron transfer from the adsorbed ions to the hydrogenated diamond (100) surfaces. The injected electrons inevitably passivate the holes in the valence band of the hydrogenated diamond (100) surface, which would thus increase electric resistance. In contrast, the HOMO and LUMO levels of the H_3O^+ ion alter significantly after adsorption. The energy levels corresponding to the HOMO and LUMO of the H_3O^+ ion both shift downwards sharply. This downward shift can be attributed to the injection of electron to the H_3O^+ ion from the hydrogenated diamond (100) surface. Consequently, electron injection result in hole accumulation in the subsurface region. Thus, the hydrogenated diamond film exhibits p-type surface conductivity [21].

From the above discussion, it can be deduced that the H_3O^+ ion in the thin water layer is important for the high surface conductivity of the hydrogenated diamond film. The gases that could increase the H_3O^+ concentration ion after dissolution into water could surely increase the surface conductivity of the hydrogenated diamond film. This may be the root explanation for the high surface conductivity of hydrogenated diamond films when exposed to gases such as NO_2 and O_3 [22, 23], as well as

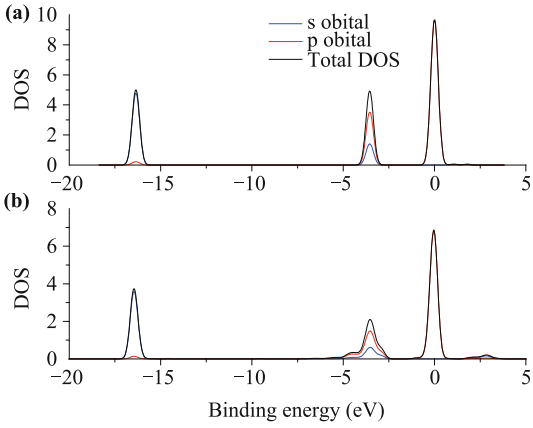

Fig. 1 The partial density of states for the **(a)** individual and **(b)** adsorptive OH^- ion.

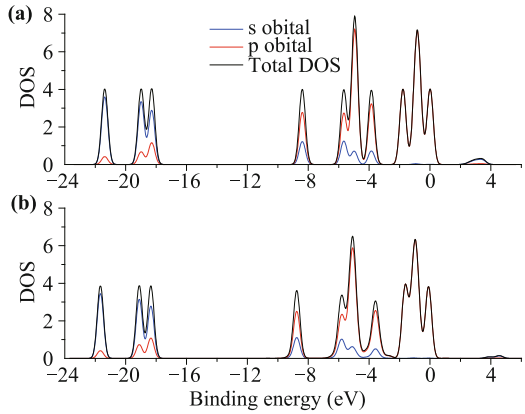

Fig. 2 The partial density of states for the **(a)** individual and **(b)** adsorptive HCO_3^- ion.

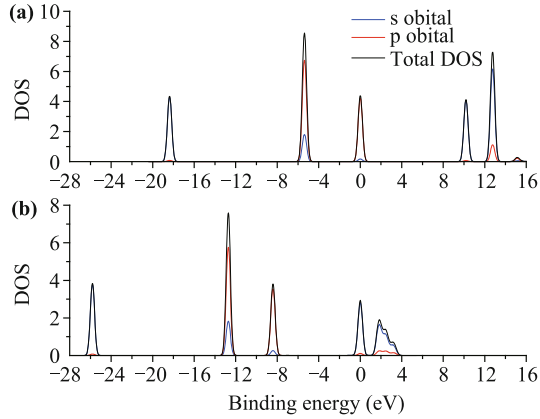

Fig. 3 The partial density of states for the **(a)** individual and **(b)** adsorptive H_3O^+ ion.

the immutability of the high surface resistance of the hydrogenated diamond film when exposed to gases like CO_2 [24]. Thus, based on the calculation results in this work, sensors sensitive to various gases that increase H_3O^+ ion concentration after dissolving into water could be developed.

4 Conclusion

After adsorption with different active ions into a thin water layer, the hydrogenated diamond (100) surface relaxes to different extents. Among the studied active ions, the H_3O^+ ion affects the geometries of the substrate most significantly due to the strong electrostatic attractions between the adsorbed ion and the hydrogenated diamond surface. In addition, electrons transfer significantly from the hydrogenated diamond (100) surface to the adsorbed H_3O^+ ion, which induces a downward shift of the H_3O^+ ion HUMO and LOMO. This has certain contributions to the high surface conductivity. However, for active ions like OH^- and HCO_3^-, no dramatic changes appear for

the electronic structures of the adsorption ions.

Acknowledgements This work was supported by the National Natural Science Foundation of China under Grant No. 51575004 and the Importation and Development of High-Caliber Talents Project of Beijing Municipal Institutions. The authors would like to thank School of Materials Science and Engineering of Tsinghua University for providing computing server.

References

1. M. I. Landstrass and K. V. Ravi, Hydrogen passivation of electrically active defects in diamond, *Appl. Phys. Lett.* 55, 1391 (1989)
2. B. Rezek, D. Shin, H. Watanabe, and C. E. Nebel, Intrinsic hydrogen-terminated diamond as ion-sensitive field effect transistor, *Sensor Actuat. B-Chem.* 122, 596 (2007)
3. C. Schreyvogel, M. Wolfer, H. Kato, M. Schreck, and C. E. Nebel, Tuned NV emission by in-plane Al-Schottky junctions on hydrogen terminated diamond, *Sci. Rep.* 4, 3634 (2014)
4. H. Kawarada, H. Sasaki, and A. Sato, Scanning-tunneling-microscope observation of the homoepitaxial diamond (001) 2×1 reconstruction observed under atmospheric pressure, *Phys. Rev. B* 52, 11351 (1995)
5. K. Hayashi, S. Yamanaka, and H. Watanabe, Investigation of the effect of hydrogen on electrical and optical properties in chemical vapor deposited on homoepitaxial diamond films, *J. Appl. Phys.* 81, 744 (1997)
6. F. B. Liu, J. D. Wang, D. R. Chen, M. Zhao, and G. P. He, The microstructures of the diamond (100) surfaces with different density of hydrogen adsorption, *Acta Phys. Sin.* 59, 6556 (2010) (in Chinese)
7. E. B. Lombardi, A. Mainwood, and K. Osuch, Interaction of hydrogen with boron, phosphorus, and sulfur in diamond, *Phys. Rev. B* 70, 205201 (2004)
8. K. Bobrov, A. J. Mayne, A. Hoffman, and G. Dujardin, Atomic-scale desorption of hydrogen from hydrogenated diamond surfaces using the STM, *Surf. Sci.* 528, 138 (2003)
9. F. Maier, M. Riedel, B. Mantel, J. Ristein, and L. Ley, Origin of surface conductivity in diamond, *Phys. Rev. Lett.* 85, 3472 (2000)
10. J. P. Goss, B. Hourahine, R. Jones, M. I. Heggie, and P. R. Briddon, p-type surface doping of diamond: a first-principles study, *J. Phys.: Condens. Matter* 13, 8973 (2001)
11. M. M. Hassan and K. Larsson, Effect of surface termination on diamond (100) surface electrochemistry, *J. Phys. Chem. C* 118, 22995 (2014)
12. V. Chakrapani, J. C. Angus, A. B. Anderson, S. D. Wolter, B. R. Stoner, and G. U. Sumanasekera, Charge transfer equilibria between diamond and an aqueous oxygen electrochemical redox couple, *Science* 318, 1424 (2007)
13. Q. X. Zhou, C. Y. Wang, Z. B. Fu, Y. J. Tang, and H. Zhang, Effects of various defects on the electronic properties of single-walled carbon nanotubes: A first principle study, *Front. Phys.* 9, 200 (2014)
14. Z. J. Ding, Y. Jiao, and S. Meng, Quantum simulation of molecular interaction and dynamics at surfaces, *Front. Phys.* 6, 294 (2011)
15. J. Furthmüller, J. Hafner, and G. Kresse, Dimer reconstruction and electronic surface states on clean and hydrogenated diamond (100) surfaces, *Phys. Rev. B* 53, 7334 (1996)
16. K. Bobrov, A. Mayne, G. Comtet, G. Dujardin, L. Hellner, and A. Hoffman, Atomic-scale visualization and surface electronic structure of the hydrogenated diamond C (100)-(2×1): H surface, *Phys. Rev. B* 68, 195416 (2003)
17. M. J. Rutter and J. Robertson, Ab initio calculation of electron affinities of diamond surfaces, *Phys. Rev. B* 57, 9241 (1998)
18. F. Maier, J. Risten, and L. Ley, Electron affinity of plasma-hydrogenated and chemically oxidized diamond (100) surfaces, *Phys. Rev. B* 64, 165411 (2001)
19. Y. Takagi, K. Shiraishi, M. Kasu, and H. Sato, Mechanism of hole doping into hydrogen terminated diamond by the adsorption of inorganic molecule, *Surf. Sci.* 609, 203 (2013)
20. H. Sato and M. Kasu, Electronic properties of H-terminated diamond during NO_2 and O_3 adsorption and desorption, *Diamond Relat. Mater.* 24, 99 (2012)
21. K. G. Girija, J. Nuwad, and R. K. Vatsa, Hydrogenated diamond as room temperature H_2S sensor, *Diamond Relat. Mater.* 40, 38 (2013)
22. S. Beer, A. Helwig, G.Müller, J. Garrido, and M. Stutzmann, Water adsorbate mediated accumulation gas sensing at hydrogenated diamond surfaces, *Sens. Actuat. B* 181, 894 (2013)
23. A. Helwig, G. Müller, J. A. Garrido, and M. Eickhoff, Gas sensing properties of hydrogen-terminated diamond, *Sens. Actuat. B* 133, 156 (2008)
24. M. Kubovic, M. Kasu, and H. Kageshima, Electronic and surface properties of H-terminated diamond surface affected by NO_2 gas, *Appl. Phys. Lett.* 96, 052101 (2010)